water

MDPI

Article

A Strontium and Hydro-Geochemical Perspective on Human Impacted Tributary of the Mekong River Basin: Sources Identification, Fluxes, and CO_2 Consumption

Shitong Zhang [1], Guilin Han [1,*], Jie Zeng [1], Xuhuan Xiao [1] and Fairda Malem [2]

[1] Institute of Earth Sciences, China University of Geosciences, Beijing 100083, China; stongzhang0103@cugb.edu.cn (S.Z.); zengjie@cugb.edu.cn (J.Z.); xiaoxuhuan@email.cugb.edu.cn (X.X.)
[2] Environmental Research and Training Center, Department of Environmental Quality Promotion, Ministry of Natural Resources and Environment, Klong Luang 12120, Thailand; mfairda@yahoo.com
* Correspondence: hanguilin@cugb.edu.cn; Tel.: +86-10-8232-3536

Abstract: As the largest and most representative tributary of the Mekong River, the Mun River Basin (MRB) provides critical understanding of regional hydro-geochemical features and rock weathering processes on a basin scale. The present study measured strontium (Sr) isotopes with hydrogeochemistry data of 56 water samples in detail in the MRB in northeast Thailand. The dissolved Sr contents and $^{87}Sr/^{86}Sr$ isotopic ratios were reported to be 8.7–344.6 µg/L (average 126.9 µg/L) and 0.7085–0.7281 (average 0.7156), respectively. The concentrations of dissolved Sr in the mainstream slightly decreased from upstream to downstream, while the variation trend of $^{87}Sr/^{86}Sr$ was on the contrary. Correlation analysis showed that Na^+ strongly correlated with Cl^- (0.995, $p < 0.01$), while Ca^{2+} exhibited weak relationships with $SO_4{}^{2-}$ (0.356, $p < 0.01$). Samples of the MRB exhibited lower Mg^{2+}/Na^+, Ca^{2+}/Na^+, $HCO_3{}^-/Na^+$ and 1000Sr/Na ratios, and gathered around the end-member of evaporite dissolution, with slight shift to silicate weathering end-member, demonstrating the dominant contribution of evaporite dissolution and silicate weathering on dissolved loads. Comparing with data of major world rivers from previous research, our results remained consistency with rivers draining through similar geological conditions. The dissolved Sr flux to the adjacent Mekong River was estimated to be 20.7 tons/year. In accordance with the forward model, silicate weathering rate and CO_2 consumption rate during dry season were calculated to be 0.73 tons/km^2/year and 1.94×10^4 mol/km^2/year, and may get underestimated due to intense water consumption by extensive agricultural activities. The superimposed effect of anthropogenic impacts on the water environment could enhance chemical weathering, and thus should be taken into account in regional ion cycles and carbon budgets. These findings highlight the coupling analysis of Sr isotopes and hydro-geochemistry in Earth surface processes and provide basic investigation for sustainable regional water treatment mechanisms in the pan basin of the Mekong River.

Keywords: strontium isotope; water chemistry; chemical weathering; Mekong tributary; Thailand; CO_2 consumption

Citation: Zhang, S.; Han, G.; Zeng, J.; Xiao, X.; Malem, F. A Strontium and Hydro-Geochemical Perspective on Human Impacted Tributary of the Mekong River Basin: Sources Identification, Fluxes, and CO_2 Consumption. *Water* **2021**, *13*, 3137. https://doi.org/10.3390/w13213137

Academic Editor: Dimitrios E. Alexakis

Received: 30 September 2021
Accepted: 5 November 2021
Published: 8 November 2021

1. Introduction

Chemical weathering serves as one major process of continental CO_2 consumption and makes a significant contribution to the biogeochemical carbon cycle [1–3]. This terrestrial process provides sufficient insights in monitoring short-time atmospheric CO_2 variation and in estimating regional climate change in the long run [4,5]. Therefore, research interest on basin geochemistry has been largely attracted to ion removal [6], weathering processes [1,7–10], their geological constraints [11–14], and the estimation of weathering and CO_2 consumption rates [15–17]. However, anthropogenic activities and atmospheric inputs could interfere with the ionic composition of rivers, making it more complicated to discriminate the controlling factors of chemical weathering processes only through the

analysis of water chemistry [12,14]. On the other hand, source characterization through the use of dissolved Sr and its radiogenic isotopes has shown to be effective in revealing weathering contribution and types to riverine solutes, especially with the correlative studies on hydrochemistry [3,12,18,19].

The Sr concentration and its isotopic ratio in the basin were principally constrained by lithological characteristics and weathering of different minerals [20]. Compared to the traditional hydro-geochemistry analysis in the river basin, radiogenic strontium isotopes ($^{87}Sr/^{86}Sr$) are far more sensitive for water sources, especially for the primary identification of chemical weathering end-member, since natural processes in the surficial environment commonly do not generate Sr isotope fractionation [21]. Therefore, strontium and its isotopes are widely used as a versatile geochemical tracer for fingerprinting weathering processes and dissolved ion provenance within the river basin. This has been demonstrated in numerous studies of the estimation on global silicate weathering rates and CO_2 consumption [5,18,22]. From a larger perspective, determination of the Sr isotopic signature of modern rivers appears to provide basic support for the estimation of riverine ion cycle within the basin.

The Mekong River is considered as a major transport channel of terrestrial materials to the reservoir of the ocean, which makes the geochemical behaviors of riverine dissolved loads an essential way in the profound investigation of terrestrial weathering [1,2]. The Mekong River is also one of the largest rivers in terms of water discharge, total length and economic significance, which extends to agriculture, hydroelectricity, navigation, and fisheries. As an essential reservoir for native organisms and local ecosystems, it provides sufficient aquatic biodiversity for local livelihood. As an important tributary of the Mekong River, the Mun River basin (MRB) belongs to a tropical monsoon climate with abundant rainfall and high temperature [23]. Published studies of the Mun River mainly focus on the riverine nutrients [24], heavy metals [25,26], dissolved organic carbon and nitrogen [23], and H−O isotopes [27], whereas the isotopic constraints of dissolved loads from Sr isotopes is rarely reported. The combination of Sr isotopes with hydro-chemistry data in the Mun River is of great significance to investigate the controlling factors of both natural chemical weathering and anthropogenic agricultural inputs [28]. Here, we report Sr concentration and its isotopic data of the Mun River water, and the main aims are as follows: (a) present the spatial distribution characteristics of water chemistry, radiogenic Sr isotopic ratios and strontium concentration of the MRB; (b) decipher in detail the source and end-member contributions of chemical weathering on Sr isotope compositions and dissolved ions, with the estimation of the relative ion flux; (c) quantify the chemical weathering and CO_2 consumption rate in the study region. This study provides basic analysis of dissolved loads on such a Mekong tributary through Sr isotope geochemistry, which benefits the management of local water resources.

2. Materials and Methods

2.1. Study Region

The Mun River Basin (MRB) is situated in the Korat Plateau of northeast Thailand (Figure 1), and is regarded as the most significant limb of the Mekong River, with a landmass of 71,060 km^2 [23] and a total length of 673 km. The elevation decreases from west to east, since mountains are encircled in the southwest of the MRB, and the middle and lower regions are distributed by the plains. The major economy sector in Thailand is agriculture due to extensive distribution of rice fields (70.8%) [29,30]. Moreover, other land use types like forests (13.5%, 14.4 million hectares) take up only a small percentage (Figure S1). The geological settings of the Mun River Basin mainly consists of semi-consolidated/unconsolidated Mesozoic and Quaternary clastic sedimentary rocks (Figure 1b), together with a small amount of igneous rocks distributed in southern Mun. Limestone only occupied for <1% of the lithology in the river basin [31,32]. Furthermore, the Mun River flows through multiple city downtowns where the urban wastewater may flow into the adjacent river. The tropical/equatorial savannah climate of study area is

significantly under the impact of southwest (SW) monsoon (May–October) and northeast (NE) monsoon (October–February), and the SW monsoon-derived precipitation generally accounts for 90% of that in total, with the variation of rainfall amount from 800 mm to 1800 mm during the rainy season and from 40 mm to 120 mm during the dry season [33–35]. Therefore, our sampling on March 2018 was located in a transition from SW to NE monsoon where the regional climate is relatively dry during the sampling period. The annual evaporation of the study region varied between 2881 mm in the west part and 5678 mm in the east [36,37], and the yearly water discharge from the Mun River to the Mekong River is about 2.5 × 10^9 m^3/year [38]. More information and descriptions of regional population, industry and climate can be obtained from our previous research [26,27].

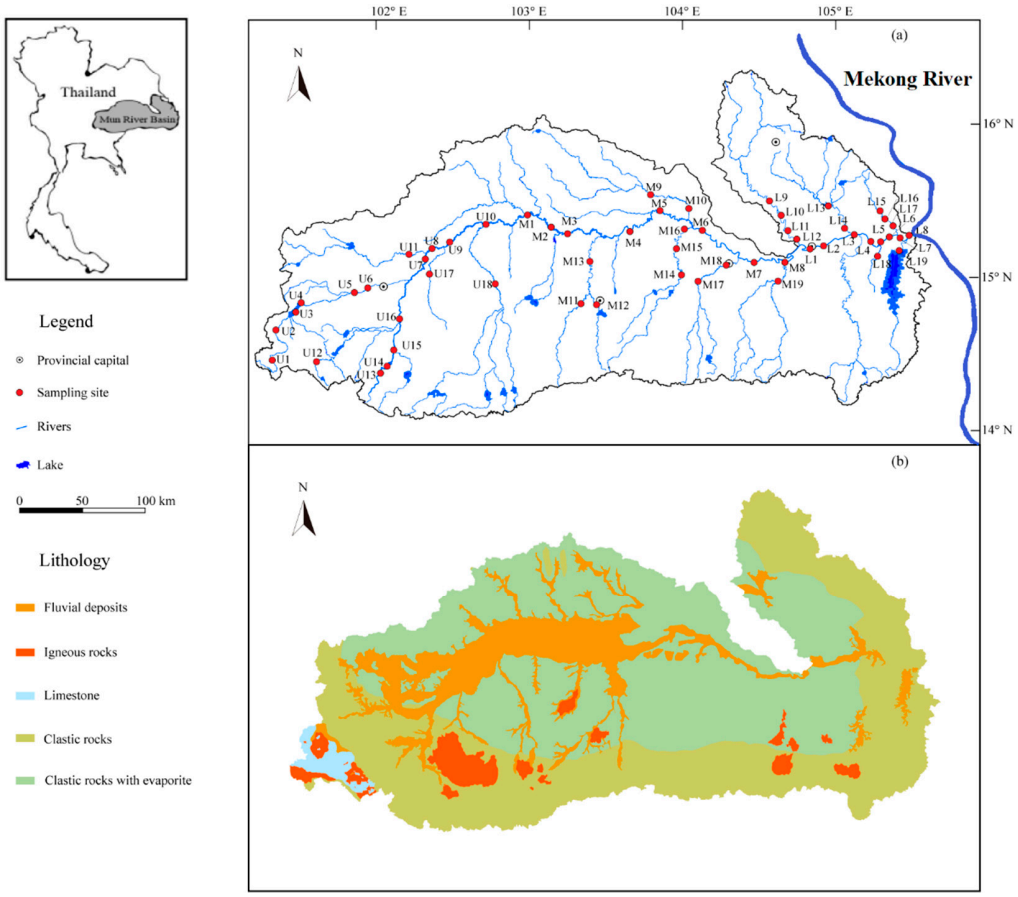

Figure 1. Maps of the Mun River Basin: (**a**) Sampling sites and geographical distribution (**b**) The geological map of the MRB.

2.2. Sampling and Chemical Analysis

Water samples of the Mun River were collected in March 2018 (dry season), and a total of 56 sampling sites were distributed along the mainstream and tributaries of the Mun River (Figure 1). The samples were denoted as U1–18, M1–19, and L1–19 for the upper, middle and lower reach, respectively, among which the samples collected from the mainstream were labelled as U1–10, M1–8, and L1–8. The remaining sites, except for that from mainstream, were all gathered from tributaries. To avoid the interference from impurities, all water samples were filtrated through a 0.22μm cellulose acetate membrane (Millipore). Samples for the measurement of major anions (HCO_3^-, Cl^-, SO_4^{2-}, NO_3^-) were then kept in the HDPE (High Density Polyethylene) bottles directly and determined by ionic chromatography (Dionex 1100, Sunnyvale, CA, USA), and that for major cations (Mg^{2+}, Ca^{2+}, K^+, and Na^+) were oxidized by ultrapure HCl to pH < 2 and determined by ICP−OES (Optima 5300DV, PerkinElmer Inc., Waltham, MA, USA). All containers were sealed and kept refrigerated at 4 °C for the following analysis in the Institute of Geographic

Sciences and Nature Resources Research, Chinese Academy of Sciences (CAS). The details in sampling procedures have been further described in our previous works [23,24].

Following the isotopic analysis method of previous research [39], water samples for strontium isotope measurement were firstly concentrated by evaporation in the oven, then separated from other dissolved ions by the standard ion-exchange techniques, and finally performed by a Nu Plasma 3 double focusing multi-collector inductively coupled plasma mass spectrometer (MC−ICP−MS, Nu Instruments, Wrexham, UK) at the Surficial Environment and Hydrological Geochemistry Laboratory in the China University of Geosciences (Beijing, China). In this study, analytical method of standard-sample bracketing (SSB) was adopted to reduce instrumental mass bias. The measured $^{87}Sr/^{86}Sr$ ratios were internally normalized by a constant $^{86}Sr/^{88}Sr$ value (0.1194) with the exponential law. The reproducibility and accuracy of Sr isotopic runs were periodically evaluated by running the standard solution NIST SRM 987 with an average isotopic ratio of 0.710276 ± 24 (2SD, N = 46).

2.3. Data Processing

A widely-used forward model was applied in this study to determine the chemical weathering sources of major ions according to mass balance equations of cations (K, Na, Ca, and Mg) from five reservoirs—precipitation, anthropogenic inputs, evaporite, silicate and carbonate [15]. For the dissolved loads in river water, the mass balance equation can be expressed as follows [2]:

$$[X]_{river} = [X]_{atmosphere} + [X]_{carbonate} + [X]_{silicate} + [X]_{evaporite} + [X]_{anthropogenic} \quad (1)$$

First, we assumed that the sample with the lowest Cl concentration value got all Cl from precipitation. Based on the $(X/Cl)_{rain}$ of local rain, the input of these four cations from precipitation can be calculated. Second, to calculate the evaporite input, we assumed that the excess Cl after precipitation correction was obtained from halite (NaCl). Third, for the estimation of silicate contribution, all Na after the correction of precipitation and evaporite and all K after the correction of precipitation were assumed to be attributed from silicate weathering. Ideally, Ca, and Mg from silicates could be estimated through data from monolithologic rivers within the study basin [15]. Fourth, the input from carbonate weathering could be calculated by subtracting the precipitation, evaporite, and silicate contributions from the total dissolved Ca and Mg in rivers. The detailed information of this model can be found in previous works [15,40].

Under such circumstances, the silicate weathering rate (SWR) within the river basin can be estimated by the sum of cations from silicate weathering, and the CO_2 consumption rate (ΦCO_2 (sili), the unit of cations is mol/L) can be calculated by the charge balance of weathering reactions as follows [41]:

$$SWR = (K_{sili} + Na_{sili} + Ca_{sili} + Mg_{sili} + SiO_2) \times Discharge/Area \quad (2)$$

$$\Phi CO_2\ (sili) = (K_{sili} + Na_{sili} + 2Ca_{sili} + 2Mg_{sili}) \times Discharge/Area \quad (3)$$

Beside this, the estimation of strontium flux in the Mun River basin provides significant insights into the transport of riverine dissolved Sr to the Mekong River, one of the large rivers in the world. Quantifying the amount of silicate-derived Sr flux obtained from weathering fractions could reflect the corresponding CO_2 degassing from solid-Earth, which may provide sufficient magnitude to alter regional climate [42]. The estimation of dissolved Sr flux of the Mun River can be derived as follows:

$$F_{Sr} = Q_{Mun} \times C_{Sr} \quad (4)$$

Here, F_{Sr} means the dissolved Sr flux from the MRB to the Mekong River, Q_{Mun} represents the river water discharge (in m^3/s), and C_{Sr} means the concentration of dissolved Sr content near the output area (in μg/L).

2.4. Software

The Pearson correlation (PC) analysis was carried out for statistics and potential ion sources identification using SPSS 26.0 (IBM Corporation, Armonk, NY, USA) and Microsoft Office 2013 (Microsoft Corporation, Redmond, WA, USA). One-way ANOVA analysis was performed to determine the significant differences of ion concentrations between river mainstream and tributaries by SPSS 26.0 (IBM Corporation, Armonk, NY, USA). All data were graphed by Origin 2017 (OriginLab Corporation, Northampton, MA, USA) and edited by CorelDRAW Graphics Suite 2018 (Corel Corporation, Ottawa, ON, CAN).

3. Results

3.1. The Spatial Distribution of Dissolved Ions and Strontium Isotopes

Table S1 illustrated the concentration of dissolved major ions, strontium, and the ratio of $^{87}Sr/^{86}Sr$ in the MRB during the sampling period selected for this study. The descriptive statistics of physicochemical parameters were presented in Table S2. The temperature in the MRB varied in a relatively small range from 24 °C to 33 °C with an average value of 28.6 °C, and the pH varied between 6.1 and 8.5 (average 7.55), indicating the neutral and alkaline river environment [24]. As presented in Figure 2a, the temperature in the lower reach of the MRB was relatively higher than the upper and middle reach, but the pH values seemed to decline from upstream to downstream. It is noteworthy that site M7 and M8 exhibited much lower pH than M6 in the mainstream (Figure 2a), since the tributaries with lowest pH values (site M17–19) converged into M7 and M8. Based on the geographical map of the MRB (Figure 1), the influence from urban discharge and domestic sewage in the provincial capital located near M18 can be regarded as a major contributor to this phenomenon.

Similar to the world average value (283 mg/L) of total dissolved solids (TDS) in rivers [43], the TDS concentrations in the MRB had an average of 269 mg/L in a broad range (13.7–1456 mg/L), reflecting the impact of land use and regional pollution [1]. In this study, the concentrations of DO displayed a rather uniform variation from 3.3 to 8.7 mg/L except for a relatively higher value in site U3 (11.8 mg/L, Table S1). The distinctive value may be attributed to stronger photosynthesis of terrestrial and aquatic plants, since site U3 was located in forest development area based on regional land use (Figure 1a and Figure S1).

The spatial variation of dissolved major ions were shown in Figure 2b,c for the whole basin and in Figure 3e–l for all tributaries in the MRB. The concentration of HCO_3^- ranged from 7.3 to 362.3 mg/L (average 78 mg/L), and that of Cl^- ranged from 1.7 to 668.5 mg/L. Moreover, the concentration of K^+ and Na^+ were 1.2–14.1 mg/L and 1.3–369.6 mg/L, respectively, and that of Ca^{2+} ranged from 1.1 to 103.5 mg/L (average 20.4 mg/L). According to ANOVA analysis of ion concentrations between mainstream and tributaries (Table S3), the concentrations of SO_4^{2-}, HCO_3^- in the upper reach showed significant differences between the tributaries and the mainstream (with the significance value of 0.032 and 0.029), and that of Na^+, Mg^{2+} and HCO_3^- in the middle reach also exhibited significant differences (with the significance value of 0.050, 0.017, and 0.006). It is noteworthy that the ion concentration in lower reach of the MRB exhibited no obvious significant differences between the mainstream and tributaries. According to our previous work [23], the mean concentration of major dissolved ions was in the order of $Cl^- > HCO_3^- > SO_4^{2-} > NO_3^-$ for anions and that of $Na^+ > Ca^{2+} > Mg^{2+} > K^+$ for cations, indicating the dominant hydrochemical type of $Na-Cl-Ca-HCO_3$ in the MRB. The contents of Na^+, K^+, SO_4^{2-} and Cl^- in the mainstream fluctuated in a similar trend from upstream to downstream, with relatively higher values in site U7–9. The concentrations of Mg^{2+}, Ca^{2+}, and HCO_3^- had a very similar decreasing trend along with the river flow. It should be noted that the contents of these major elements were relatively lower after the junction of the middle and lower reaches (site M8 and L1), which was mainly as a result of the additional dilution effect in river discharge from the convergence of tributaries (site L9–12) and the uniform distribution in regional geology (Figure 1).

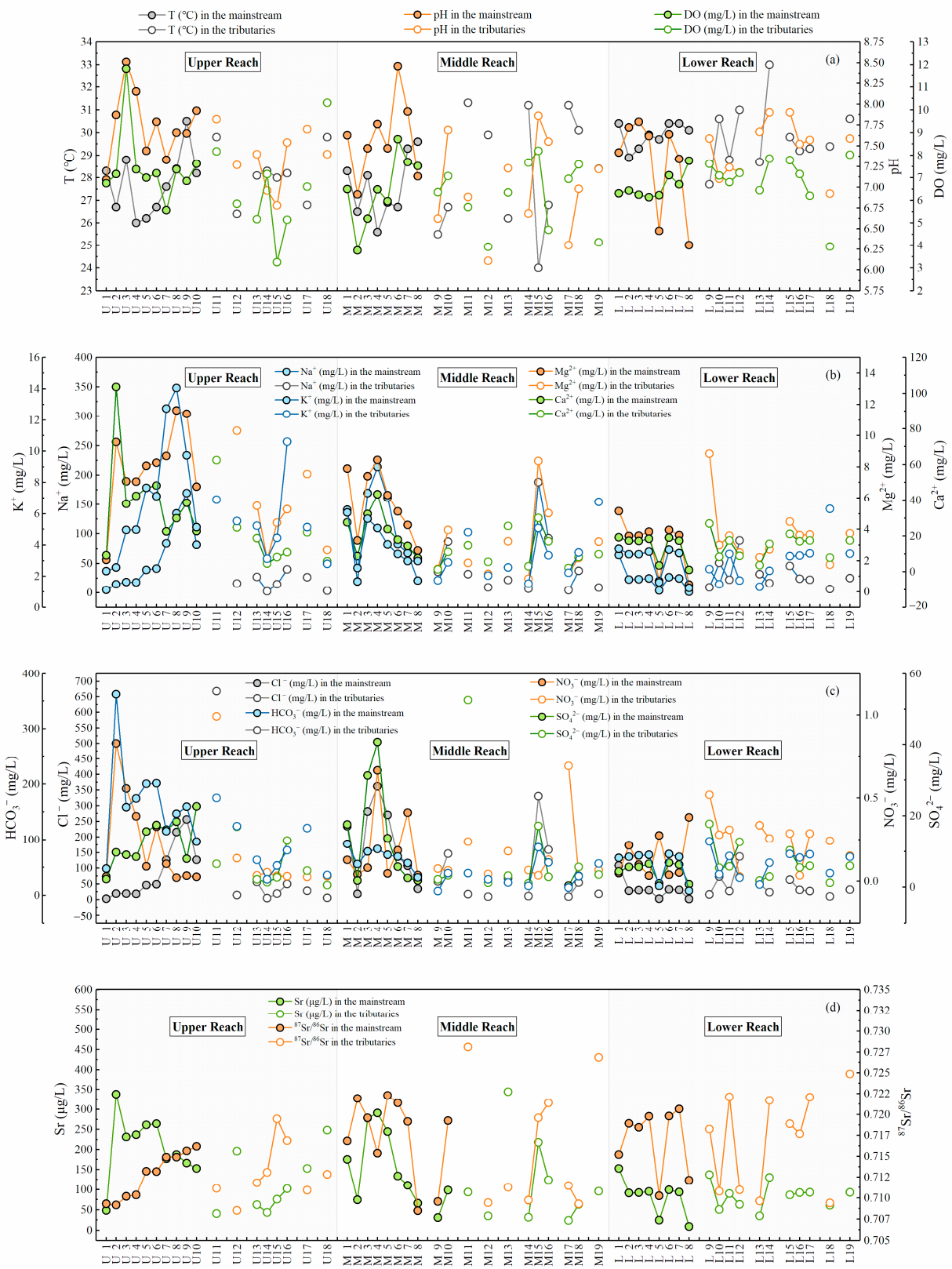

Figure 2. The spatial variation diagram of (**a**) temperature, pH, EC, and DO; (**b**) the concentration of major dissolved cations; (**c**) the concentration of major dissolved anions; (**d**) Sr concentration and $^{87}Sr/^{86}Sr$ in the Mun River.

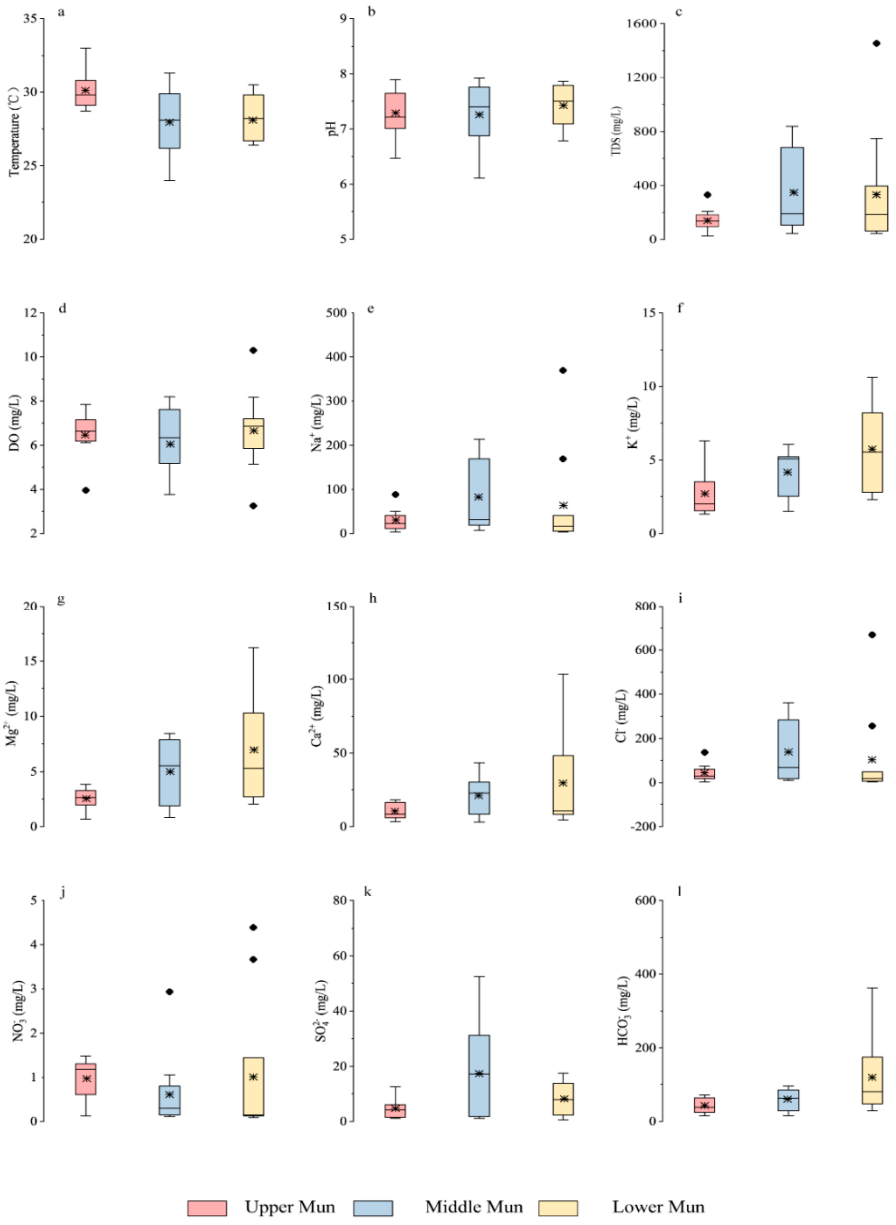

Figure 3. Box plots of (**a**) temperature (**b**) pH (**c**) TDS (**d**) DO in the MRB and the concentration of (**e**) Na^+ (**f**) K^+ (**g**) Mg^{2+} (**h**) Ca^{2+} (**i**) Cl^- (**j**) $NO_3{}^-$ (**k**) $SO_4{}^{2-}$ (**l**) $HCO_3{}^-$ in the MRB tributaries. Note that ● represented the respective outliers, and * represented the mean values.

In addition, in comparison with the guideline values of drinking water quality by the World Health Organization [44], it is obvious that the total chlorine (Cl^-) contents in the Mun River were much higher than the guideline values (3 mg/L), which may be attributed to wide distribution of evaporites in the basin. The nitrate ($NO_3{}^-$) contents of water samples were much lower than the guideline values (11 mg/L), indicating no significant threat to drinking water health. $NO_3{}^-$ contents in the mainstream existed several higher values in the lower reach (Figures 2c and 3), which may be ascribed to potential anthropogenic pollutions near the sampling sites (fertilizer, sewage and industrial wastewater) [24].

As shown in Tables S1 and S2, the dissolved Sr contents in the MRB ranged from 8.7 to 344.6 µg/L with an average of 126.9 µg/L, higher than the world average (78.3 µg/L) [45]. The concentrations of dissolved Sr in the mainstream slightly decreased from upstream to downstream, while the variation trend of $^{87}Sr/^{86}Sr$ was on the contrary (Figure 2d and Table S2). According to the ANOVA analysis (Table S3), the dissolved Sr concentrations

in the upper reach showed significant differences between the tributaries and the mainstream (with the significance value of 0.025). However, dissolved Sr contents in the other two reaches did not exhibit the same, indicating no significant variation between mainstream and tributaries downstream. The ratio of dissolved $^{87}Sr/^{86}Sr$ ranged from 0.7085 to 0.7281, similar to that in the Seine River (0.7077–0.7168, Le Havre, France) [2] draining a typical Mesozoic−Cenozoic sedimentary basin under temperate climatic conditions, and that in the Indus River (0.7098–0.7120) [46] draining though sedimentary carbonates under tropical climate. However, it is generally lower than that in Himalayan rivers (0.7115–0.9646) [21], draining mostly through silicate bedrocks. The mean value of Sr isotopic ratios (0.7156) is similar to that of the world average (0.7119) [45]. Comparing to the upper and middle reach in the MRB, the lower reach exhibited relatively large fluctuations of radiogenic Sr isotopes from 0.709 to 0.725, indicating the potential impact of tributary lithology due to concentrated distribution in the lower reach, and also to the impact of the water mixing process near the Mekong River. Moreover, it is worth noting that site U15, U16, M11, and M19 exhibited much higher $^{87}Sr/^{86}Sr$ values than that in adjacent tributaries within the watershed, which is probably because of the draining through silicate bedrocks according to regional lithology (Figure 1).

3.2. The Source of Dissolved Ions and Strontium Isotopes

To study the chemical relationships among the variables of the river water samples, the statistical techniques of Pearson correlation analysis was applied. Figure 4 presented the hot map of Pearson correlation coefficients in selected parameters measured in the MRB. It is obvious that Na^+ strongly correlated with Cl^- (0.995, $p < 0.01$), and Ca^{2+} exhibited weak relationships with SO_4^{2-} (0.356, $p < 0.01$). In addition, HCO_3^- showed strong positive correlation between Ca^{2+} (0.935, $p < 0.01$) and Mg^{2+} (0.764, $p < 0.01$).

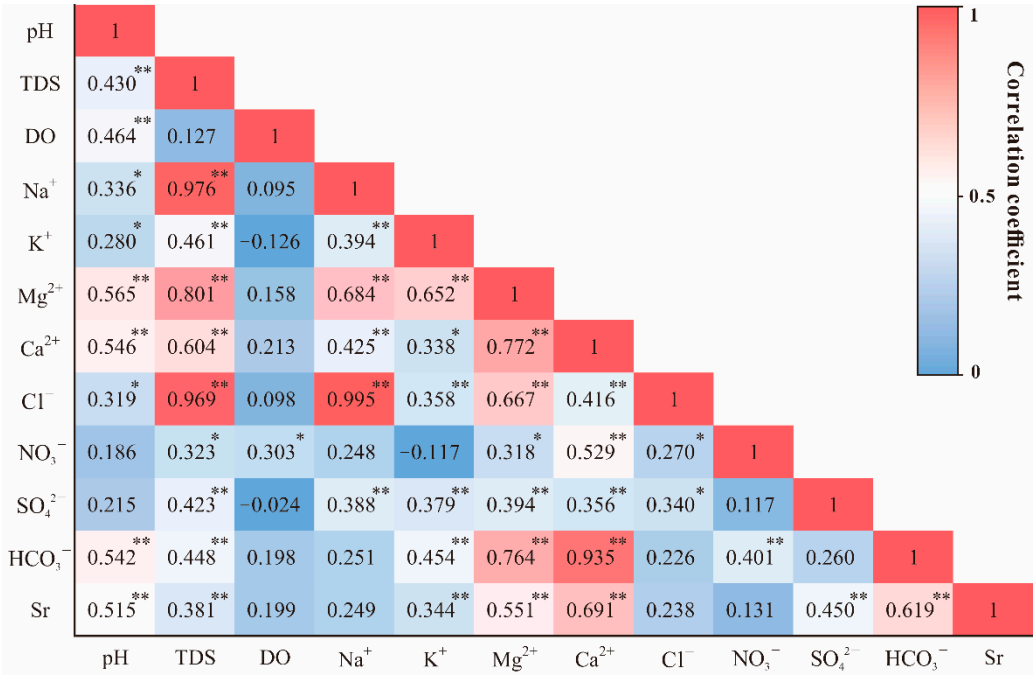

Figure 4. Pearson correlation coefficients of selected parameters measured in the MRB. * Correlation is significant at $p < 0.05$ level; ** Correlation is significant at $p < 0.01$ level.

The elemental ratios of Ca^{2+}/Na^+ versus HCO_3^-/Na^+ and Mg^{2+}/Na^+ were plotted in Figure 5 to reflect the controlling factors of weathering source (evaporites, silicates and carbonates). The water samples were located among three fundamental end-members and much closer to the evaporite-silicate end-members, confirming the mixing contributions between different weathering products. When compared with data of 61 world

rivers derived from previous research [1], samples of the MRB have lower molar ratios of Mg^{2+}/Na^{+}, Ca^{2+}/Na^{+} and HCO_3^{-}/Na^{+}; this likely reflects the dominant impact of evaporite dissolution. Moreover, it can be seen in Figure 5 that water samples in the upper Mun seemed much closer to the silicate weathering end-member, whereas the influence of evaporite dissolution was strengthened more in the middle reach. Beside this, some sampling points plotted particularly far away from the range of these end-members, indicating the additional contribution from other potential inputs.

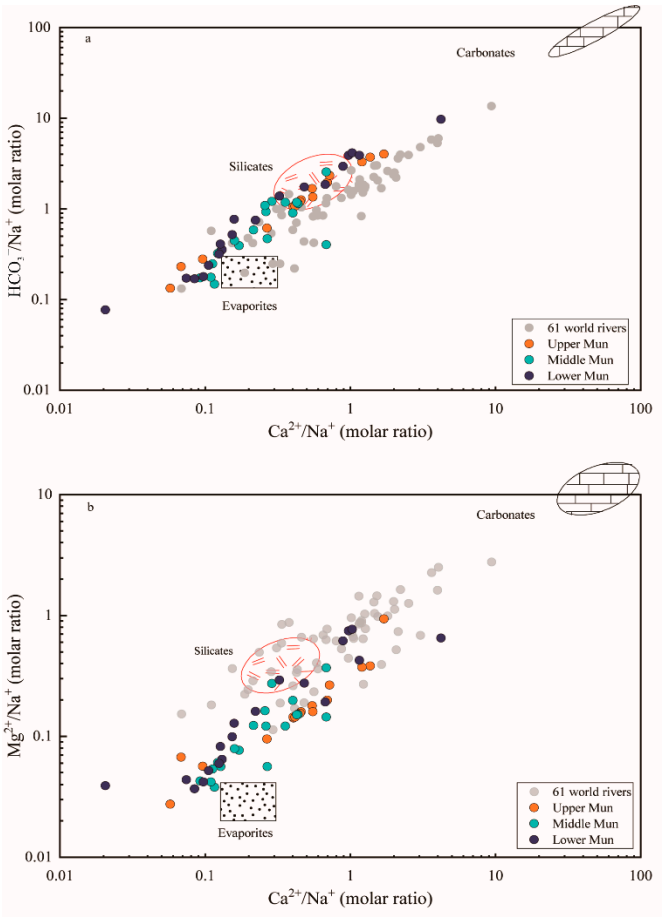

Figure 5. The elemental ratio of (**a**) HCO_3^{-}/Na^{+} and (**b**) Mg^{2+}/Na^{+} versus Ca^{2+}/Na^{+} molar ratios of waters samples in the MRB and the world major rivers. The data of 61 large world rivers and three end-members were derived from [1].

From the correlation analysis mentioned above in Figure 4, strontium has a relatively strong correlation with Ca^{2+} in the river water (0.691, $p < 0.01$), which exists more clearly when plotting the Na-normalized ratios of Ca/Na and 1000Sr/Na together ($R^2 = 0.76$, Figure 6). This correlation supports the mixing processes between evaporites and silicates (lower Sr/Na and Ca/Na ratios). Furthermore, the plotted ratios in lower reach appeared centralized in the most left corner of the figure than the upper reach, indicating the divergence of contribution in distinct parts of the basin. It should also be noted that the plot of site U18 (located in one of the large tributaries in the MRB) deviated from the fitting line, indicating the additional alteration by other potential controlling factors. According to previous studies of strontium in world rivers [1], evaporites have much lower Sr/Na and Ca/Na ratios compared to silicates and carbonates. Considering the other major world rivers dominated by various lithology [1], our results remained consistency with the rivers draining through similar geological conditions, such as the Mekong river (Figure 6).

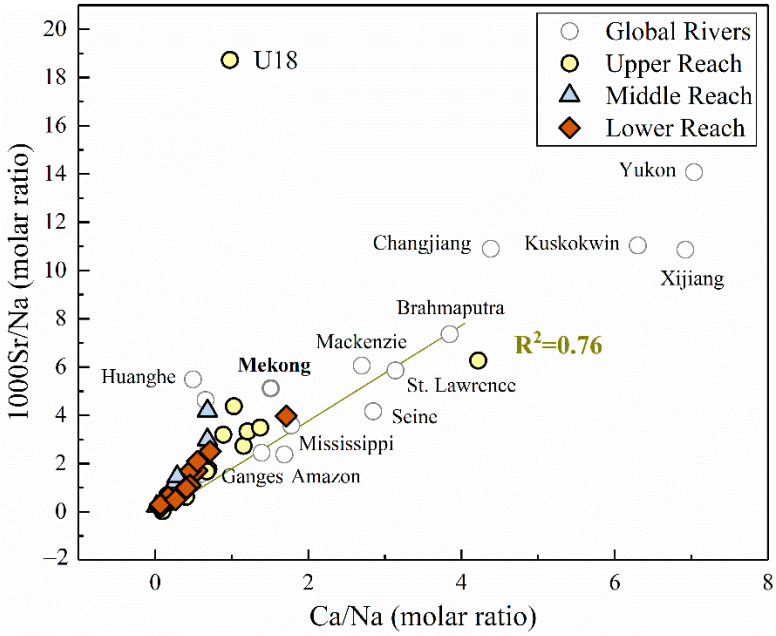

Figure 6. The molar ratio of 1000Sr/Na versus Ca/Na in the MRB and other large rivers around the world (gray hollow dots). Data of major world rivers were derived from [1].

Figure 7a exhibited the mixing plot of $^{87}Sr/^{86}Sr$ vs. 1/Sr in the upper, middle and lower part of the MRB, and no significant relationship existed between these two ratios. Water samples fanned out towards lower Sr isotopic ratios rather than falling on the same trend, implying the multi end-member mixing of strontium isotopes along the river flow instead of a traditional mixing process mentioned above. As shown in Figure 7b, the plotted samples obviously gathered around the end-member of evaporite dissolution and slightly shifted towards the end-member of silicate weathering. In terms of the individual part of divided reaches, the upper reach deviated a little towards the carbonate end-member, while the middle and lower reach exhibited much more centralized to the mixing line between evaporites and silicates.

3.3. The Sr Flux, Chemcial Weathering and Related CO_2 Consumption Rate

The relative contributions of rock weathering on dissolved Sr can be discriminated by the following Equation [42]:

$$\left(\frac{^{87}Sr}{^{86}Sr}\right)_{riv} = \left(\frac{^{87}Sr}{^{86}Sr}\right)_{rain} \times Sr_{rain} + \left(\frac{^{87}Sr}{^{86}Sr}\right)_{carb} \times Sr_{carb} + \left(\frac{^{87}Sr}{^{86}Sr}\right)_{evap} \times Sr_{evap} + \left(\frac{^{87}Sr}{^{86}Sr}\right)_{sili} \times Sr_{sili} \quad (5)$$

The $(^{87}Sr/^{86}Sr)_{riv}$, $(^{87}Sr/^{86}Sr)_{rain}$, $(^{87}Sr/^{86}Sr)_{carb}$, $(^{87}Sr/^{86}Sr)_{evap}$, and $(^{87}Sr/^{86}Sr)_{sili}$ represent the $^{87}Sr/^{86}Sr$ ratios of the Mun River, regional rainwater, carbonates, evaporites and silicates, respectively. Sr_{rain}, Sr_{carb}, Sr_{evap}, and Sr_{sili} indicate the contribution proportions of each potential reservoirs. Based on several assumptions and conditions discussed below (Section 4.1), the results can be drawn that the proportion of evaporite dissolution interpreted mostly the dissolved Sr in the MRB (average 63%, ranged 18–99%). The segment of silicate weathering occupied the other 37% in average which ranged from 1% to 82%. For the upper reach of the Mun River, evaporite dissolution made the most significant contribution (average 80%) to the riverine Sr compared to the middle (average 51%) and lower reach (average 57%), while the silicate weathering contributed most to the dissolved Sr in the middle reach (average 49%).

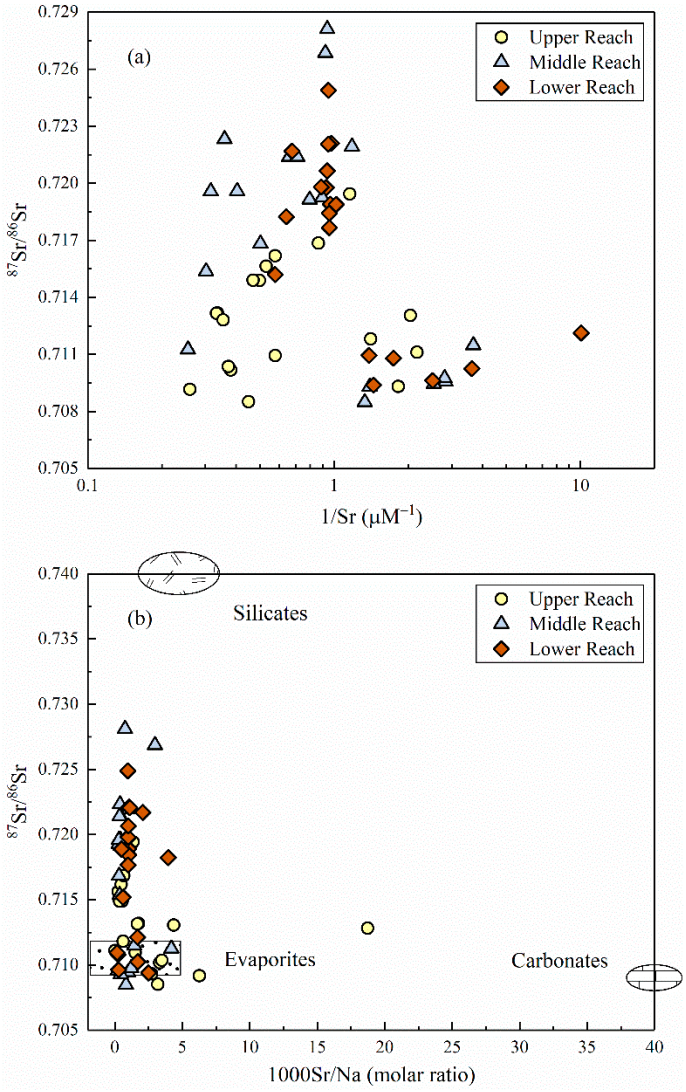

Figure 7. (**a**) $^{87}Sr/^{86}Sr$ ratios versus 1/Sr (**b**) $^{87}Sr/^{86}Sr$ ratios versus 1000Sr/Na molar ratios in the MRB. Data of the end-members (evaporites, silicates and carbonates) were referred from [47].

According to the hydrological data provided by Royal Irrigation Department of Thailand (R.I.D) and the identical Sr output from the MRB, the dissolved Sr flux to the Mekong River was thus calculated to be 20.7 tons/year in the dry season based on Equation (4), providing a certain contribution to the dissolved Sr into world's large rivers. A simplified calculation of weathering and related CO_2 consumption rate was conducted based on appropriate assumptions (see details in Section 4.2). The results showed that the silicate weathering rates of the MRB during dry season was 0.73 tons/km^2/year, and the value of CO_2 consumption rate was calculated to be 1.94×10^4 mol/km^2/year.

4. Discussion

4.1. Contributions of Chemical Weathering to Dissolved Ions

4.1.1. Weathering Source Identification of Dissolved Ions

As for the bedrock weathering source, the potential process affecting riverine solutes could be regarded as follows: (a) the dissolution of evaporite [48], which contains gypsum dissolution (introducing Ca^{2+} and SO_4^{2-}) and halite dissolution (introducing Na^+ and Cl^-), (b) the dissolution of silicate minerals by CO_2, which brings Si, HCO_3^-, K^+, Na^+, Mg^{2+} and Ca^{2+}, (c) the dissolution of carbonates by CO_2, which introduces Mg^{2+}, Ca^{2+} and HCO_3^- into the river. As shown in Figure 4, it is obvious that the strong correlation between Na^+

and Cl^- (0.995, $p < 0.01$) indicated the possible presence of halite dissolution within the river basin, which is also consistent with regional geological settings (Figure 1). However, weak relationships between Ca^{2+} and $SO_4{}^{2-}$ (0.356, $p < 0.01$) implied less significant contributions from gypsum dissolution. The strong positive correlation between $HCO3^- - Ca^{2+}$ (0.935, $p < 0.01$) and $HCO_3{}^- - Mg^{2+}$ (0.764, $p < 0.01$) indicated the potential weathering of silicates within southern MRB, since the river hardly drained through carbonate area (Figure 1).

Furthermore, the elemental ratios of Ca^{2+}/Na^+ versus $HCO_3{}^-/Na^+$ and Mg^{2+}/Na^+ could primarily reflect the controlling factors of bedrock weathering on major dissolved ions due to the variations between the weathering of evaporites, silicates and carbonates [1,49]. The three major reservoirs could be discriminated separately as (a) evaporites (halite): $Ca^{2+}/Na^+ = 0.2$, $HCO_3{}^-/Na^+ = 0.12$, $Mg^{2+}/Na^+ = 0.012$, (b) silicates: $Ca^{2+}/Na^+ = 0.35 \pm 0.15$, $HCO_3{}^-/Na^+ = 2 \pm 0.1$, $Mg^{2+}/Na^+ = 0.24 \pm 0.12$, (c) carbonates: $Ca^{2+}/Na^+ = 50$, $HCO_3{}^-/Na^+ = 120$, $Mg^{2+}/Na^+ = 10$ based on previous studies on large world rivers [1]. Similar trends were observed in the MRB as shown in Figure 5, confirming the mixing contributions between different weathering products, principally the dissolution of evaporites and silicate rocks [1]. Therefore, evaporite weathering (dissolution) may be one of the most important controlling factors dominating dissolved loads in the Mun river water, and silicate weathering could be suggested as another potential contributor of riverine solutes.

It has been widely accepted that $HCO_3{}^-$, Mg^{2+}, and Ca^{2+} are not strongly affected by anthropogenic factors, while Na^+ is partly controlled by pollution [12]. As mentioned above, the large population in provincial capitals and the extensive agriculture distribution in Thailand result in the largest land use of crop fields within the MRB. Therefore, the anthropogenic inputs, especially agricultural activities and urban wastes, may also lead to the deviated values of measured chemical parameters and play a significant role in the contribution of dissolved solutes, such as $SO_4{}^{2-}$, and $NO_3{}^-$. Beside the above hypotheses, the regional climate during the sampling period was in a transition from southwest (SE) to northeast (NE) tropical monsoons [23], and the precipitation in the rainy season (southwest monsoon) accounted for nearly 90% of the annual precipitation [24]; the effect of precipitation during sampling period (dry season) can thus be neglected compared to other times of the year. According to our previous work on hydrogen and oxygen isotopes [27], it is possible that the surface evaporation also made a potential contribution to water chemistry and dissolved ions in the MRB, since the evaporation line of the Mun River in dry season ($\delta^2H = 5.27 \times \delta^{18}O - 15.76$, $n = 56$, $R^2 = 0.91$) was significantly lower than that of the local meteoric water line (LMWL, $\delta^2H = 7.68 \times \delta^{18}O + 7.25$, $n = 56$, $R^2 = 0.91$) of Bangkok. This is consistent with the basic environmental conditions (tropical climate, high temperature and scarce precipitation in dry season) for evaporation. Under such circumstances, in the next section the combined usage of strontium isotopes with hydrochemistry characteristics will help further identify the relative end-member contributions from weathering processes, and provide a much concrete view on riverine dissolved loads.

4.1.2. Potential End-Member Contribution of Strontium

The radiogenic strontium isotope ($^{87}Sr/^{86}Sr$) compositions of river waters commonly exhibit identical signatures draining through different bedrock lithology and rarely fractionates during natural biogeochemical processes, and thus has been extensively applied to the study field of elemental material cycle in the catchment scale [19,50,51]. Previous studies have discriminated two distinct pathways for the variation of riverine Sr contents and $^{87}Sr/^{86}Sr$ ratios: silicate weathering with typically lower Sr concentration and higher isotopic ratios, and vice versa for river draining through carbonate bedrocks [18]. As shown in Figure 7b, the relationship of $^{87}Sr/^{86}Sr$ versus 1000Sr/Na molar ratios of the Mun River clearly demonstrated the mixing trends between evaporites and silicates [47]. In terms of the individual part of divided reaches, the upper reach could be explained by the appearance of limestone adjacent to the headwater of the Mun River, and the middle and lower reach corroborated the hypothesis of chemical weathering sources derived

from the analysis of hydro-geochemistry. Therefore, the dissolved loads in the MRB is primarily controlled by the weathering of evaporite dissolution and a small amount of silicate weathering.

The quantification of end-member contribution to strontium is indispensable prior to the estimation of Sr flux to the adjacent Mekong River and CO_2 degassing through silicate weathering [18]. As previously noted, rainfall amount within the basin varied from 800–1800 mm during the wet season [33], and from 40–120 mm in the dry season [35]. Therefore, the precipitation in the dry season was neglected, since rainfall in the wet season generally accounts for nearly 92–98% of the total annual precipitation (that is, only 2–8% for the dry season) [38,52]. Moreover, considering the wide distribution of the clastic sedimentary rock basement and the coverage of thick quaternary alluvial deposits [31,38], and that the carbonates (limestones) only distributed in the limited area of the westernmost tip of the basin (Figure 1), the contribution of carbonate weathering in this region was assumed negligible for the simplification of our calculation. The commonly representative values of 0.710 [47] for evaporite dissolution contribution were also adopted in our calculations. According to regional geological settings (Figure 1), the sampling site M11 with the highest $^{87}Sr/^{86}Sr$ ratio (0.7281) drained obviously through silicate bedrocks, thus was regarded as an appropriate constraint of silicate end-member in the formula. Therefore, the equation mentioned above can be simplified as:

$$\left(\frac{^{87}Sr}{^{86}Sr}\right)_{riv} = Sr_{evap} \times 0.710 + Sr_{sili} \times 0.7281 \quad (6)$$

In addition to the simple two end-member mixing equation based on mass balance (Sr_{evap} + Sr_{sili} = 1), the results can be drawn when eliminating several deviated values due to the factors neglected previously in our calculation. The calculation results strongly confirmed that the major contributor of dissolved loads in the Mun River via natural processes should be evaporite dissolution foremost and silicate weathering the second.

4.1.3. Estimation of Dissolved Sr Flux

Since the water samples available for dissolved Sr flux calculation were collected in dry season, the corresponding river discharge and dissolved Sr concentration were applied to the estimation (see Section 2.3 for more info). Our previous work [23] has demonstrated no obvious annual variation of river runoff in the MRB, and the average annual runoff at the M.11B hydrological station located at the outlet of the MRB is 2.6×10^{10} m^3. According to the hydrological data provided by Royal Irrigation Department of Thailand (R.I.D), the water discharge during our sampling periods reached to 75 m^3/s in the lower Mun [38], which occupied about 9.1% of the total annual runoff in the MRB. In detail, the Sr concentration of site L8 (8.7 μg/L) was selected to represent the identical Sr output from the MRB, as it was located in the most downstream site in the lower Mun. For the sake of simplification in the calculation, we assumed that the detected values during sampling period remain consistent. On the basis of such circumstances, the dissolved Sr flux to the Mekong River was thus calculated to be 20.7 tons/year in the dry season, providing a certain contribution to the dissolved Sr into world's large rivers. Furthermore, the relative flux of ^{87}Sr in excess of seawater Sr isotope composition (generally consistent to 0.709) was also calculated as follows [20]:

$$^{87}Sr_{excess}flux = \left(\frac{^{87}Sr}{^{86}Sr} - 0.709\right) \times \text{Total } Sr_{flux} \quad (7)$$

The result was calculated to be 0.06 tons of ^{87}Sr each year in excess to the Mekong River from the MRB and finally to the adjacent ocean, indicating the potential influence of the Mun River on seawater Sr isotope evolution.

4.2. Influencing Factors of Chemical Weathering and Related CO_2 Consumption Rate

Chemical weathering makes continental denudation significant to geochemical cycles, since riverine solutes are continuously transported into the large reservoir of ocean. Weath-

ering reactions within the river basin indirectly consume CO_2, making the weathering rate essential for controlling the long-term CO_2 concentrations in the atmosphere and alter global temperature of surficial environment in the long run [2]. The major silicate weathering reactions are as follows [53]:

$$2NaAlSi_3O_8 + 2CO_2 + 11H_2O \rightarrow Al_2Si_2O_5(OH)_4 + 2HCO_3^- + 2Na^+ + 4H_4SiO_4 \quad (8)$$

$$2KAlSi_3O_8 + 2CO_2 + 6H_2O \rightarrow Al_2Si_4O_{10}(OH)_2 + 2HCO_3^- + 2K^+ + 2H_4SiO_4 \quad (9)$$

$$CaAl_2Si_2O_8 + 2CO_2 + 3H_2O \rightarrow Al_2Si_2O_5\left(OH\right)_4 + 2HCO_3^- + Ca^{2+} \quad (10)$$

$$Mg_2SiO_4 + 4CO_2 + 4H_2O \rightarrow 4HCO_3^- + 2Mg^{2+} + H_4SiO_4 \quad (11)$$

Moreover, not all chemical weathering reactions involve CO_2, as major evaporate minerals (NaCl, $CaSO_4$, and $CaSO_4 \cdot xH_2O$) dissolve without reacting with acids except water. Since no prominent contribution of carbonate weathering was observed, we only calculated silicate weathering rates and CO_2 consumption rates in this paper.

Here, a forward model was applied to estimate the amount of major dissolved ions for the calculation of silicate weathering rate and CO_2 consumption (see more details in Section 2.3) [1,15]. A simplified calculation was conducted based on the following assumptions. First, since the precipitation during sampling period generally accounts for only 2–8% of the total annual precipitation [38], we neglect the effect of atmospheric inputs ($[X]_{atmosphere}$), and also ignore the inputs from carbonate weathering due to limited distribution. Secondly, evaporite (halite) dissolution should act as a dominant source of Na^+ and Cl^- in the MRB, since the influence from sea salt is weak in inland rivers, and these two ions showed highly positive correlations (Figure 4) with wide distribution and significant impact of evaporite dissolution. Therefore, it is appropriate to make the assumption that the minimum value of Cl^- (1.7 mg/L) in the MRB was totally originated from evaporite (halite) dissolution ($[Cl]_{min} = [Cl]_{evap} = [Na]_{evap}$). Furthermore, contrary what is seen in large natural rivers like the Congo and the Amazon [1], the MRB is apparently impacted by anthropogenic activities such as agriculture and urban industry (Figure S1). Anthropogenic activities commonly related to K^+, Na^+, Cl^-, NO_3^-, and SO_4^{2-}. For anthropogenic-originated chlorine, the $[Cl]_{anth}$ (17.8 mg/L) can thus be obtained by subtracting evaporite Cl from riverine Cl ($[Cl]_{river}$ = 19.5 mg/L).The simplified equations can be written as follows [15,54]:

$$[Cl]_{min} = [Cl]_{evap} \quad (12)$$

$$[Cl]_{river} = [Cl]_{evap} + [Cl]_{anth} \quad (13)$$

$$[Ca]_{river} = [Ca]_{sili} + [Ca]_{evap} \quad (14)$$

$$[Mg]_{river} = [Mg]_{sili} + [Mg]_{anth} \quad (15)$$

$$[K]_{river} = [K]_{sili} + [K]_{anth} \quad (16)$$

$$[Na]_{river} = [Na]_{sili} + [Na]_{evap} + [Na]_{anth} \quad (17)$$

For the sake of relatively accurate estimation, the average value of dissolved loads in site L4–8 which located in the mainstream closest to the river mouth were regarded as the outlet concentrations of each dissolved ion. Hence, the mean value of SiO_2 in this sites (6.9 mg/L) was applied to our calculation. For anthropogenic-originated K and Na, the reference value of anthropogenic inputs ($[K]_{anth}$ = 1.4 mg/L, $[Na]_{anth}$ = 3.6 mg/L) can be derived from the Cl^--normalized ratios of K and Na in agricultural activities (K/Cl = 0.08, Na/Cl = 0.2) [2]. Then, the remainder of K and Na after the correction anthropogenic and evaporite inputs were regarded as the main products originated from silicate weathering ($[K]_{sili}$ = 1.3 mg/L, $[Na]_{sili}$ = 10.7 mg/L). Ideally, Ca, and Mg from silicates should be estimated through data from monolithologic rivers within the local region. However, due to the absence of appropriate data in the MRB, the Na-normalized ratios of Ca and Mg compiled from typical silicate bedrocks (Ca/Na = 0.44, Mg/Na = 0.16) were chosen in our

calculation [15]. Therefore, silicate-derived Ca and Mg were calculated to be 4.7 mg/L for $[Ca]_{sili}$ and 1.7 mg/L for $[Mg]_{sili}$, respectively.

According to the above analysis, the calculated silicate weathering rates of the MRB during dry season was 0.73 tons/km^2/year, and the value of CO_2 consumption rate was 1.94×10^4 mol/km^2/year. Assuming that SWR remains consistent on terrestrial surface environment, the CO_2 sink by silicate weathering in dry season was calculated to be 1.65×10^{-8} Gt C/year. In addition, water consumption by agricultural tillage along the river would cut down river runoff to some extent, and further give rise to the underestimation of weathering rate and CO_2 consumption. Considering the extensive distribution of rice fields and agricultural activities in the MRB, this could be a potential determinant affecting the estimation and may require further in-depth investigation.

In summary, as shown in our discussion, the anthropogenic activities in the Mekong tributary, especially agriculture, played an important role in altering regional chemical weathering and subsequent transportation process. From another perspective, anthropogenic impacts such as agriculture and industry could accelerate chemical weathering by introducing protons into the river water, since recent works in the pan basin of the Mekong River have demonstrated the significant pollution of human activities on dissolved sulfate [29], nitrogen [38] and riverine nutrients [24]. Beyond that, let alone the whole Mekong River, any one of the tributaries (the MRB) could act as a primary source of drinkable water and agricultural production for more than 10 million people. As such, more systematic research on regional climate change and human health may provide a comprehensive view for better agricultural management along the river. The establishment of relative water treatment should also be highly recommended and carried out to develop a long-term monitoring mechanism near the Mekong River.

5. Conclusions

This study focused on source identification and distribution characteristics of riverine Sr and hydro-geochemistry in the Mun River under natural and anthropogenic impacts. The dissolved Sr concentrations and $^{87}Sr/^{86}Sr$ ratios were reported to be 8.7–344.6 μg/L (higher than world average) and 0.7085–0.7281 (similar to world average), respectively. The dissolved Sr values and $^{87}Sr/^{86}Sr$ ratios in the mainstream were higher than that in the tributaries. Correlation analysis along with Sr isotopes demonstrated the primary contribution of evaporite dissolution and silicate weathering on dissolved loads. According to the two-member mixing model, the proportion of evaporite dissolution accounted for more than half of dissolved Sr (average 63%), indicating the predominance of evaporite dissolution within the basin. The dissolved Sr flux to the Mekong River was calculated to be 20.7 tons/year in the dry season, providing a certain contribution into one of the world's largest rivers. The silicate weathering rate and the CO_2 consumption rate were calculated to be 0.73 tons/km^2/year and 1.94×10^4 mol/km^2/year, respectively. Considering extensive agricultural activities in the MRB, the above calculation may be underestimated due to reduced river runoff and intense consumption by agriculture along the river. Although the regional CO_2 sink by silicate weathering seemed to be much smaller than that in major reservoirs, it may still be taken into account in the regional carbon budgets. Natural processes, together with the addition of anthropogenic activities, enhance the coupled transport of dissolved loads and make it necessary to develop long-term monitoring mechanisms and water treatment schemes in the major tributary of the Mekong River.

Supplementary Materials: The following are available online at https://www.mdpi.com/article/10.3390/w13213137/s1, Figure S1: Land use and statistical data of agriculture/industry change in the MRB. Table S1: The concentration of dissolved ions and strontium isotopes in the Mun River. Table S2: Descriptive statistics of the detected physicochemical parameters in the MRB. Table S3: The results of One-way ANOVA analysis on detected chemical parameters in the MRB.

Author Contributions: Conceptualization, S.Z. and G.H.; Formal analysis, S.Z. and G.H.; Funding acquisition, G.H.; Methodology, S.Z., J.Z. and G.H.; Resources, G.H.; Software, S.Z., X.X. and G.H.;

Supervision, G.H.; Validation, S.Z., J.Z. and G.H.; Visualization, S.Z., J.Z., G.H. and X.X.; Writing—original draft, S.Z., G.H., J.Z., X.X. and F.M.; Writing—review & editing, S.Z. and G.H. All authors have read and agreed to the published version of the manuscript.

Funding: This research was funded jointly by the National Natural Science Foundation of China (No. 41661144029; 41325010). This research was also funded by the 2021 Graduate Innovation Fund Project of China University of Geosciences, Beijing (No. YB2021YC018).

Institutional Review Board Statement: Not applicable.

Informed Consent Statement: Not applicable.

Data Availability Statement: The data presented in this study are available on request from the corresponding author.

Acknowledgments: The authors gratefully acknowledge Chao Song, Qian Zhang, and teammates from the Ministry of Natural Resource and Environment of Thailand for the assistance of field sampling.

Conflicts of Interest: The authors declare no conflict of interest.

References

1. Gaillardet, J.; Dupré, B.; Louvat, P.; Allegre, C. Global silicate weathering and CO_2 consumption rates deduced from the chemistry of large rivers. *Chem. Geol.* **1999**, *159*, 3–30. [CrossRef]
2. Roy, S.; Gaillardet, J.; Allegre, C. Geochemistry of dissolved and suspended loads of the Seine river, France: Anthropogenic impact, carbonate and silicate weathering. *Geochim. Cosmochim. Acta* **1999**, *63*, 1277–1292. [CrossRef]
3. Dalai, T.K.; Krishnaswami, S.; Kumar, A. Sr and $^{87}Sr/^{86}Sr$ in the Yamuna River System in the Himalaya: Sources, fluxes, and controls on Sr isotope composition. *Geochim. Cosmochim. Acta* **2003**, *67*, 2931–2948. [CrossRef]
4. Millot, R.; Gaillardet, J.; Dupré, B.; Allègre, C.J. The global control of silicate weathering rates and the coupling with physical erosion: New insights from rivers of the Canadian Shield. *Earth Planet. Sci. Lett.* **2002**, *196*, 83–98. [CrossRef]
5. Boral, S.; Peucker-Ehrenbrink, B.; Hemingway, J.D.; Sen, I.S.; Galy, V.; Fiske, G.J. Controls on short-term dissolved $^{87}Sr/^{86}Sr$ variations in large rivers: Evidence from the Ganga–Brahmaputra. *Earth Planet. Sci. Lett.* **2021**, *566*, 116958. [CrossRef]
6. Uiga, K.; Tenno, T.; Zekker, I.; Tenno, T. Dissolution modeling and potentiometric measurements of the SrS–H_2O–gas system at normal pressure and temperature at salt concentrations of 0.125–2.924 mM. *J. Sulfur Chem.* **2011**, *32*, 137–149. [CrossRef]
7. Chen, L.; Liu, J.; Zhang, W.; Zhou, J.; Luo, D.; Li, Z. Uranium (U) source, speciation, uptake, toxicity and bioremediation strategies in soil-plant system: A review. *J. Hazard. Mater.* **2021**, *413*, 125319. [CrossRef]
8. Zeng, J.; Han, G. Tracing zinc sources with Zn isotope of fluvial suspended particulate matter in Zhujiang River, southwest China. *Ecol. Indic.* **2020**, *118*, 106723. [CrossRef]
9. Wang, J.; Wang, L.; Wang, Y.; Tsang, D.C.W.; Yang, X.; Beiyuan, J.; Yin, M.; Xiao, T.; Jiang, Y.; Lin, W.; et al. Emerging risks of toxic metal(loid)s in soil-vegetables influenced by steel-making activities and isotopic source apportionment. *Environ. Int.* **2021**, *146*, 106207. [CrossRef]
10. Qin, C.; Li, S.-L.; Waldron, S.; Yue, F.-J.; Wang, Z.-J.; Zhong, J.; Ding, H.; Liu, C.-Q. High-frequency monitoring reveals how hydrochemistry and dissolved carbon respond to rainstorms at a karstic critical zone, Southwestern China. *Sci. Total Environ.* **2020**, *714*, 136833. [CrossRef]
11. Mortatti, J.; Probst, J.-L. Silicate rock weathering and atmospheric/soil CO_2 uptake in the Amazon basin estimated from river water geochemistry: Seasonal and spatial variations. *Chem. Geol.* **2003**, *197*, 177–196. [CrossRef]
12. Chetelat, B.; Liu, C.Q.; Zhao, Z.Q.; Wang, Q.L.; Li, S.L.; Li, J.; Wang, B.L. Geochemistry of the dissolved load of the Changjiang Basin rivers: Anthropogenic impacts and chemical weathering. *Geochim. Cosmochim. Acta* **2008**, *72*, 4254–4277. [CrossRef]
13. Han, G.; Tang, Y.; Liu, M.; Van Zwieten, L.; Yang, X.; Yu, C.; Wang, H.; Song, Z. Carbon-nitrogen isotope coupling of soil organic matter in a karst region under land use change, Southwest China. *Agric. Ecosyst. Environ.* **2020**, *301*, 107027. [CrossRef]
14. Xu, S.; Li, S.; Su, J.; Yue, F.; Zhong, J.; Chen, S. Oxidation of pyrite and reducing nitrogen fertilizer enhanced the carbon cycle by driving terrestrial chemical weathering. *Sci. Total Environ.* **2021**, *768*, 144343. [CrossRef]
15. Moon, S.; Huh, Y.; Qin, J.; van Pho, N. Chemical weathering in the Hong (Red) River basin: Rates of silicate weathering and their controlling factors. *Geochim. Cosmochim. Acta* **2007**, *71*, 1411–1430. [CrossRef]
16. Liu, J.; Han, G. Controlling factors of riverine CO_2 partial pressure and CO_2 outgassing in a large karst river under base flow condition. *J. Hydrol.* **2021**, *593*, 125638. [CrossRef]
17. Wang, W.; Li, S.-L.; Zhong, J.; Wang, L.; Yang, H.; Xiao, H.; Liu, C.-Q. CO_2 emissions from karst cascade hydropower reservoirs: Mechanisms and reservoir effect. *Environ. Res. Lett.* **2021**, *16*, 044013. [CrossRef]
18. Singh, S.K.; Kumar, A.; France-Lanord, C. Sr and $^{87}Sr/^{86}Sr$ in waters and sediments of the Brahmaputra river system: Silicate weathering, CO_2 consumption and Sr flux. *Chem. Geol.* **2006**, *234*, 308–320. [CrossRef]
19. Stevenson, R.; Pearce, C.R.; Rosa, E.; Hélie, J.-F.; Hillaire-Marcel, C. Weathering processes, catchment geology and river management impacts on radiogenic ($^{87}Sr/^{86}Sr$) and stable ($\delta^{88}/^{86}Sr$) strontium isotope compositions of Canadian boreal rivers. *Chem. Geol.* **2018**, *486*, 50–60. [CrossRef]

20. Bickle, M.J.; Bunbury, J.; Chapman, H.J.; Harris, N.B.; Fairchild, I.J.; Ahmad, T. Fluxes of Sr into the headwaters of the Ganges. *Geochim. Cosmochim. Acta* **2003**, *67*, 2567–2584. [CrossRef]
21. Oliver, L.; Harris, N.; Bickle, M.; Chapman, H.; Dise, N.; Horstwood, M. Silicate weathering rates decoupled from the $^{87}Sr/^{86}Sr$ ratio of the dissolved load during Himalayan erosion. *Chem. Geol.* **2003**, *201*, 119–139. [CrossRef]
22. Zieliński, M.; Dopieralska, J.; Belka, Z.; Walczak, A.; Siepak, M.; Jakubowicz, M. Sr isotope tracing of multiple water sources in a complex river system, Noteć River, central Poland. *Sci. Total Environ.* **2016**, *548–549*, 307–316. [CrossRef]
23. Li, X.; Han, G.; Liu, M.; Song, C.; Zhang, Q.; Yang, K.; Liu, J. Hydrochemistry and Dissolved Inorganic Carbon (DIC) Cycling in a Tropical Agricultural River, Mun River Basin, Northeast Thailand. *Int. J. Environ. Res. Public Health* **2019**, *16*, 3410. [CrossRef]
24. Liu, J.; Han, G.; Liu, X.; Liu, M.; Song, C.; Yang, K.; Li, X.; Zhang, Q. Distributive Characteristics of Riverine Nutrients in the Mun River, Northeast Thailand: Implications for Anthropogenic Inputs. *Water* **2019**, *11*, 954. [CrossRef]
25. Liang, B.; Han, G.; Liu, M.; Li, X.; Song, C.; Zhang, Q.; Yang, K. Spatial and Temporal Variation of Dissolved Heavy Metals in the Mun River, Northeast Thailand. *Water* **2019**, *11*, 380. [CrossRef]
26. Zeng, J.; Han, G.; Yang, K. Assessment and sources of heavy metals in suspended particulate matter in a tropical catchment, northeast Thailand. *J. Clean. Prod.* **2020**, *265*, 121898. [CrossRef]
27. Yang, K.; Han, G. Controls over hydrogen and oxygen isotopes of surface water and groundwater in the Mun River catchment, northeast Thailand: Implications for the water cycle. *Hydrogeol. J.* **2020**, *28*, 1021–1036. [CrossRef]
28. Zhou, W.; Han, G.; Liu, M.; Li, X. Effects of soil pH and texture on soil carbon and nitrogen in soil profiles under different land uses in Mun River Basin, Northeast Thailand. *PeerJ* **2019**, *7*, e7880. [CrossRef] [PubMed]
29. Liu, J.; Han, G. Tracing riverine sulfate source in an agricultural watershed: Constraints from stable isotopes. *Environ. Pollut.* **2021**, *288*, 117740. [CrossRef] [PubMed]
30. Liu, M.; Han, G.; Li, X. Contributions of soil erosion and decomposition to SOC loss during a short-term paddy land abandonment in Northeast Thailand. *Agric. Ecosyst. Environ.* **2021**, *321*, 107629. [CrossRef]
31. Han, G.; Yang, K.; Zeng, J.; Zhao, Y. Dissolved iron and isotopic geochemical characteristics in a typical tropical river across the floodplain: The potential environmental implication. *Environ. Res.* **2021**, *200*, 111452. [CrossRef]
32. Liu, M.; Han, G.; Li, X. Using stable nitrogen isotope to indicate soil nitrogen dynamics under agricultural soil erosion in the Mun River basin, Northeast Thailand. *Ecol. Indic.* **2021**, *128*, 107814. [CrossRef]
33. Prabnakorn, S.; Maskey, S.; Suryadi, F.; de Fraiture, C. Rice yield in response to climate trends and drought index in the Mun River Basin, Thailand. *Sci. Total Environ.* **2018**, *621*, 108–119. [CrossRef]
34. Peel, M.C.; Finlayson, B.L.; McMahon, T.A. Updated world map of the Köppen-Geiger climate classification. *Hydrol. Earth Syst. Sci.* **2007**, *11*, 1633–1644. [CrossRef]
35. Zhao, Z.; Liu, G.; Liu, Q.; Huang, C.; Li, H. Studies on the spatiotemporal variability of river water quality and its relationships with soil and precipitation: A case study of the Mun River Basin in Thailand. *Int. J. Environ. Res. Public Health* **2018**, *15*, 2466. [CrossRef] [PubMed]
36. Akter, A.; Babel, M.S. Hydrological modeling of the Mun River basin in Thailand. *J. Hydrol.* **2012**, *452–453*, 232–246. [CrossRef]
37. Liang, B.; Han, G.; Liu, M.; Li, X. Zn isotope fractionation during the development of low-humic gleysols from the Mun River Basin, northeast Thailand. *Catena* **2021**, *206*, 105565. [CrossRef]
38. Liu, X.-L.; Han, G.; Zeng, J.; Liu, M.; Li, X.-Q.; Boeckx, P. Identifying the sources of nitrate contamination using a combined dual isotope, chemical and Bayesian model approach in a tropical agricultural river: Case study in the Mun River, Thailand. *Sci. Total Environ.* **2021**, *760*, 143938. [CrossRef]
39. Li, X.; Han, G. One-step chromatographic purification of K, Ca, and Sr from geological samples for high precision stable and radiogenic isotope analysis by MC-ICP-MS. *J. Anal. At. Spectrom.* **2021**, *36*, 676–684. [CrossRef]
40. Li, X.; Han, G.; Liu, M.; Yang, K.; Liu, J. Hydro-Geochemistry of the River Water in the Jiulongjiang River Basin, Southeast China: Implications of Anthropogenic Inputs and Chemical Weathering. *Int. J. Environ. Res. Public Health* **2019**, *16*, 440. [CrossRef]
41. Wu, W.; Zheng, H.; Yang, J.; Luo, C.; Zhou, B. Chemical weathering, atmospheric CO_2 consumption, and the controlling factors in a subtropical metamorphic-hosted watershed. *Chem. Geol.* **2013**, *356*, 141–150. [CrossRef]
42. Wang, Z.L.; Zhang, J.; Liu, C.Q. Strontium isotopic compositions of dissolved and suspended loads from the main channel of the Yangtze River. *Chemosphere* **2007**, *69*, 1081–1088. [CrossRef] [PubMed]
43. Han, G.; Liu, C.-Q. Water geochemistry controlled by carbonate dissolution: A study of the river waters draining karst-dominated terrain, Guizhou Province, China. *Chem. Geol.* **2004**, *204*, 1–21. [CrossRef]
44. World Health Organization. Guidelines for Drinking-Water Quality: Fourth Edition Incorporating the First Addendum. 2017. Available online: https://www.who.int/publications/i/item/9789241549950 (accessed on 5 July 2021).
45. Palmer, M.; Edmond, J. The strontium isotope budget of the modern ocean. *Earth Planet. Sci. Lett.* **1989**, *92*, 11–26. [CrossRef]
46. Karim, A.; Veizer, J. Weathering processes in the Indus River Basin: Implications from riverine carbon, sulfur, oxygen, and strontium isotopes. *Chem. Geol.* **2000**, *170*, 153–177. [CrossRef]
47. Negrel, P.; Allègre, C.J.; Dupré, B.; Lewin, E. Erosion sources determined by inversion of major and trace element ratios and strontium isotopic ratios in river water: The Congo Basin case. *Earth Planet. Sci. Lett.* **1993**, *120*, 59–76. [CrossRef]
48. Li, X.; Han, G.; Liu, M.; Liu, J.; Zhang, Q.; Qu, R. Potassium and its isotope behaviour during chemical weathering in a tropical catchment affected by evaporite dissolution. *Geochim. Cosmochim. Acta* **2021**, *316*, 105–121. [CrossRef]

49. Millot, R.; érôme Gaillardet, J.; Dupré, B.; Allègre, C.J. Northern latitude chemical weathering rates: Clues from the Mackenzie River Basin, Canada. *Geochim. Cosmochim. Acta* **2003**, *67*, 1305–1329. [CrossRef]
50. Palmer, M.; Edmond, J. Controls over the strontium isotope composition of river water. *Geochim. Cosmochim. Acta* **1992**, *56*, 2099–2111. [CrossRef]
51. Han, G.; Tang, Y.; Xu, Z. Fluvial geochemistry of rivers draining karst terrain in Southwest China. *J. Asian Earth Sci.* **2010**, *38*, 65–75. [CrossRef]
52. Li, R.; Huang, H.; Yu, G.; Yu, H.; Bridhikitti, A.; Su, T. Trends of runoff variation and effects of main causal factors in Mun River, Thailand During 1980–2018. *Water* **2020**, *12*, 831. [CrossRef]
53. Liu, J.; Han, G. Major ions and $\delta^{34}S_{SO4}$ in Jiulongjiang River water: Investigating the relationships between natural chemical weathering and human perturbations. *Sci. Total Environ.* **2020**, *724*, 138208. [CrossRef] [PubMed]
54. Xu, Z.; Liu, C.-Q. Chemical weathering in the upper reaches of Xijiang River draining the Yunnan–Guizhou Plateau, Southwest China. *Chem. Geol.* **2007**, *239*, 83–95. [CrossRef]